ARTICLE

Characterization of C12A7-O^- Catalyst and Mechanism of Phenol Formation by Hydroxylation of Benzene

Ting Dong, Zhao-xiang Wang, Tao Kan, Quan-xin Li*

Department of Chemical Physics, Lab of Biomass Clean Energy, University of Science and Technology of China, Hefei 230026, China

(Dated: Received on August 29, 2006; Accepted on December 4, 2006)

The benzene conversion and phenol selectivity from $C_6H_6/O_2/H_2O$ over $[Ca_{24}Al_{28}O_{64}]^{4+}\cdot 4O^-$(C12A7-$O^-$) catalyst were investigated using a flow reactor. The benzene conversion increases with the increase of temperature, and the phenol selectivity mainly depends on both reaction temperature and the composition of the mixtures. The changes of the catalyst structure before and after the reactions and the intermediates on the catalyst surface and in the bulk were investigated by XRD, EPR and FT-IR. The catalytic reactions do not cause any damage to the structure of the positively charged lattice framework C12A7-O^-, but part of the O^- and $O_2{}^-$ species in the bulk of C12A7-O^- translate to OH^- after the reactions. The neutral species and anion intermediate were investigated by Q-MS and TOF-MS respectively. It is suggested that the active O^- and OH^- species played a key role in the process of phenol formation.

Key words: Benzene, Phenol, C12A7-O^-, O^-, OH^-

I. INTRODUCTION

Phenol, one of the most important chemical products, is an important intermediate chemical for the production of antioxidants, agrochemicals, dyes, medicines, and polymers. Currently, phenol is mainly produced by the so-called cumene process and toluene oxidation process [1]. The cumene process consists of three reactions: alkylation of benzene, oxidation of cumene and decomposition of cumene hydroperoxide. The toluene oxidation process also consists of two reactions: oxidation of toluene and oxidative decomposition of benzoic acid. Some problems exist for both processes. The drawbacks of the cumene process, for example, are the co-production of acetone and the formation of small amounts of byproducts (e.g. n-propylbenzene and di-isopropylbenzene) which interfere in the separation steps. In the toluene oxidation process, the low yields of the two reactions should be improved. Therefore, direct synthesis of phenol from benzene has attracted considerable attention and remains one of the important challenges in the industrial chemistry.

The most promising results in direct hydroxylation of benzene have been explored with N_2O as oxidant with various metal oxides by Iwamoto *et al.* in 1983 [2], and, so far, with ZSM-5 zeolites or different ZSM-5 modifications as catalysts [3-5]. When benzene was oxygenated with nitrous oxide over Fe-ZSM-5 catalyst [6-8], at 330 °C and 25% conversion of benzene, the selectivity to phenol formation was more than 99%. Nitrous oxide decomposes leaving so-called active oxygen inside the pore system of ZSM-5 zeolites [9,10]. Benzene reacts directly with the active oxygen forming phenol. The drawback of this catalytic system is that the production capacity of phenol depends on a source of waste nitrous oxide like the adipic acid plant.

Also, some interesting results have been obtained in the hydroxylation of benzene with hydrogen peroxide or with an oxygen/hydrogen mixture, using zeolites modified with metals or noble metals as catalysts [11-13], e.g., titanium-silicate (TS-1) zeolites [14] and Pd membrane [15]. Kunai *et al.* reported that phenol was obtained by hydroxylation of benzene with oxygen and hydrogen with almost 100% selectivity on Cu-Pd/SiO_2 catalyst at 60 °C and under atmospheric pressure [16]. But using an oxygen-hydrogen mixture in a large-scale synthesis is not preferred. Using oxygen as oxide, preferably air, is the most attractive catalytic system for direct synthesis of phenol because it is the cheapest one and involves no environmental pollution.

The compound $12CaO\cdot 7Al_2O_3$ (C12A7), one of the crystalline phases in the system of $CaCO_3$ and Al_2O_3, is a major constituent in aluminous cements, and in recent years, a number of studies have been reported on it [17-19]. Recently, it has been found that C12A7 can be transformed into C12A7-O^- ($[Ca_{24}Al_{28}O_{64}]^{4+}\cdot 4O^-$) under certain conditions [17,19]. For microporous C12A7-O^-, the O^- anions can be stored in the cages of C12A7-O^- and can also be emitted into the gas phase by applying an extraction field under suitable temperature [18,19]. Furthermore, in many reports O^- plays an important role in catalytic oxidation reactions [20-28]. Because of the unique O^- storage and emission behavior of C12A7-O^-, this material can be used as a good catalyst to oxygenate or decompose some chemicals (e.g. hydrocarbons). For example, C12A7 has been used as a catalyst in partial oxidation of methane to syngas [29].

*Author to whom correspondence should be addressed. E-mail: liqx@ustc.edu.cn

 ©2007 Chinese Physical Society

More recently, we found the C12A7-O^- catalyst was active in steam reforming of bio-oil, and give a hydrogen yield close to thermodynamic equilibrium [30,31].

In our previous communication [32], a direct synthesis of phenol from benzene with oxygen and water over the microporous material C12A7-O^- as a stable catalyst was reported, and the effects of temperature, oxygen concentration and water on the benzene conversion, and selectivity of phenol were investigated [32]. In this work, to make clear the synthesis mechanism of phenol and further increase the phenol yield, the surface reactions on C12A7-O^- were investigated in a low-pressure reactor (∼133 μPa). The formed intermediates, the structure changes before and after the phenol synthesis, and the active species both in the body and on the surface of the catalyst were investigated by a series of characterization methods.

II. EXPERIMENTS

A. C12A7-O^- preparation

The C12A7-O^- catalyst was prepared by a solid-state reaction at a high temperature. Powders of $CaCO_3$ and γ-Al_2O_3 were mixed and ground at a molar ratio of $CaCO_3$:γ-Al_2O_3=12:7. The powder mixture was pressed to a pellet with a diameter of 15 mm and a thickness of 1.5 mm. Then it was sintered at 1573 K for 18 h and cooled to the room temperature under flowing dry oxygen atmosphere. Afterwards the sintered pellets were ground into powder (250-350 μm), which was used as a catalyst for benzene conversion.

B. Phenol synthesis

Phenol synthesis from benzene/oxygen/water was performed in a flow type reactor at 101 kPa. Typically, the reactor, containing 3 g of the C12A7-O^- catalyst on the surface of an inner quartz tube (16 mm o.d.) was connected to an ice-cooling condenser. Benzene bubbled by argon gas or other mixed gas was fed to the catalyst between the inner and outer tubes (the gap: 2.5 mm). The temperature was measured by a thermocouple placed near the heater around the outer tube. The temperature had been calibrated by another thermocouple placed in the catalyst. The reactants and products were analyzed by two on-line gas chromatographs (GC1 and GC2). Benzene (before and after reaction) and the products besides CO and CO_2 were detected by GC1. Products of CO and CO_2 were detected by GC2. Ar/O_2 and $Ar/O_2/H_2O$ together with electrons (supplied by a negative dc power with a current of 0.3-0.4 mA) were fed to the catalyst. The neutral species desorbed from C12A7-O^- surface in the formation process of phenol were also measured with a quadrupole mass spectrometer (Balzers, GSD 300 OmniStar).

C. Characterization of the catalyst

XRD measurements were employed to investigate the structure difference between the initial C12A7-O^- catalysts and the used C12A7-O^- catalysts after the phenol synthesis. The catalysts were generally crushed into powder with the average diameter of 20-30 μ m. Powder X-ray diffraction patterns were recorded on an X'pert Pro Philips diffractometer with a Cu-Kα source. The measurement conditions were in the 2θ range of 10°-80°, step counting time of 5 s, and step size of 0.017° at at 298 K.

EPR measurements (electron paramagnetic resonance) were performed to investigate the oxygen species in the bulk C12A7-O^-. The EPR measurements were conducted at ∼9.1 GHz (X-band) using a Bruker ER-200D spectrometer at 77 K. The concentrations of the oxygen species in the C12A7-O^- were determined from the second integral of the spectrum using $CuSO_4 \cdot 5H_2O$ as a standard with an error of about 20%.

Fourier transform infrared (FT-IR) spectra were used to study the active species on the catalyst surface, and measured at 298 K by a Bruker EQUINOX55 FT-IR spectrometer with KBr pellet method. The catalysts for FT-IR measurements were mixed at a weight ratio of catalyst:KBr=100:3, then ground and pressed by a pressure of 40.4 MPa to a pellet with a diameter of at 1 cm and a thickness of 0.3 mm. The infrared absorption spectra were recorded and analyzed.

D. Analysis of surface reactions and intermediates

The experimental apparatus for studying the surface reactions and the emission has been described previously [32,33]. Briefly, it is made up of two major parts: a reaction chamber and a detection chamber with a time of flight mass spectrometer (TOF-MS) for anion measurements, which is individually pumped by two turbo molecular pumps. The C12A7-O^- catalyst was supported by a ship-like quartz tube, which was mounted in the center of the reaction chamber. The heater was quartz-sealed in order to avoid the possible influence of electrons emitted from it beyond our observation. The reaction temperature was measured by a Ni/Cr thermocouple. The anionic products desorbed from the catalyst surface were extracted by an extraction electrode, and detected by TOF-MS. The background vacuum of the catalyst chamber was pumped to <0.1 mPa. The reactants (e.g. benzene or other mixtures) were fed onto the front-side surface (the side facing the TOF spectrometer) of the C12A7-O^- by a nozzle with a variable pressure range of 0.1-100 mPa. In addition, the neutral species desorbed from the C12A7-O^- surface in

DOI:10.1088/1674-0068/20/03/297-304 ©2007 Chinese Physical Society

TABLE I The effect of temperature on the benzene conversion, product selectivity, and phenol yield over the C12A7-O^- catalyst

T/°C	Conversion/%	S/%		Yield/(mmol/g_{cat}·h)
		C_6H_5OH	$CO+CO_2$	
200	<0.5	100.0	0	<0.020
250	1.1	94.6	5.4	0.045
278	2.7	69.1	30.9	0.098
350	10.1	83.0	17.0	0.346
421	26.2	81.6	18.4	0.883
492	15.3	83.1	16.7	0.525
528	24.5	88.0	11.7	0.891
565	33.3	89.3	10.5	1.230
600	40.1	78.2	21.3	1.295
635	44.0	83.2	15.7	1.512
671	39.9	80.6	17.6	1.329
707	46.0	78.2	20.3	1.486

Reaction conditions: C_6H_6:O_2:H_2O:Ar=0.08:0.04:0.19:0.69, implantation current: 0.35 mA, flow rate: 63 mL/min, pressure: 101 kPa, C12A7-O^- : 3g. Benzene conversion was based on the amount of benzene introduced into the reactor. The product selectivity was based on the benzene reacted.

the formation process of phenol were measured with a quadrupole mass spectrometer (Balzers, GSD 300 OmniStar).

III. RESULTS AND DISCUSSION

A. Performance of phenol synthesis on C12A7-O^- catalyst

The benzene conversion over the C12A7-O^- catalyst mainly depends on the reaction temperature. The phenol selectivity and yield are mainly affected by the reaction temperature and the composition of the feeding mixture (i.e., the ratio of C_6H_6:O_2:H_2O). Table I shows the temperature effect on benzene conversion and phenol selectivity with the optimum mixtures (C_6H_6:O_2:H_2O=2:1:4.8, C_6H_6=10.1 kPa) over the C12A7-O^- catalyst. It was found that phenol was the dominant product, and the major by-products were CO and CO_2, which were produced by the decomposition and oxidation of benzene over the C12A7-O^- catalyst. No benzene conversion was observed at temperatures lower than 200 °C. With increasing temperature, the benzene conversion significantly increases, but the phenol selectivity shows a maximum value at around 550 °C. The conversion of benzene and the phenol selectivity were c lose to 34% and 90% respectively with a gas mixture of C_6H_6:O_2:H_2O:Ar=0.08:0.04:0.19:0.69 over the catalyst at 565 °C. The phenol yield was about 1.26±0.16 mmol/g_{cat}·h, and remained nearly constant within the tested interval of 1000 min. It was found that carbon deposition was negligible after 1000 min's reaction. This can be attributed to the presence of O_2 and H_2O, which restrained the coke formation.

According to our previous work, it has been identified that the amount of the desorbed active O^- radicals increased with increasing reaction temperature. When the temperature rises from 500 °C to 800 °C, the emitted O^- current density increases more than three orders of magnitude (from nA/cm^2 level to μA/cm^2 level) [19]. Accordingly, the concentration of O^- anions on the C12A7 surface should increase with the increasing temperature, which may lead to the increase of the catalytic activities for benzene conversion. On the other hand, when water was fed, some OH^- anions was generated from the reaction: $O^-(s)+H_2O(s) \rightarrow OH^-(s)+OH(s)$ [33]. Moreover, the role of water in the reaction system may enhance hydroxylation of benzene by increasing OH^- concentration, and so inhibit the consecutive oxidation of phenol. For example, the phenol selectivity increased from 75% to near 90% on increasing the concentration of water from 0 to 12% at a given O_2 concentration of 4.5% at 565 °C. As shown below, the active species of $O^-(s)$ and $OH^-(s)$ should play an important role in the phenol formation over the C12A7-O^- catalyst.

B. Structure characteristics of C12A7-O^-

XRD measurement was employed to investigate the structure difference between the initial C12A7-O^- catalyst and the reacted C12A7-O^- catalyst for phenol synthesis. The peaks in Fig.1 that are marked by "*" are assigned to the lattice framework of C12A7 by comparing the peak positions and intensities of the XRD pattern with the data in the JCPDS cards. There

DOI:10.1088/1674-0068/20/03/297-304 ©2007 Chinese Physical Society

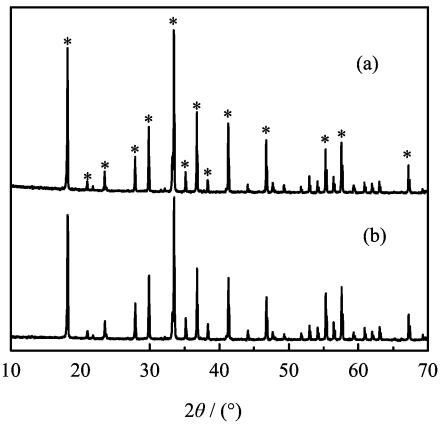

FIG. 1 XRD patterns of (a) the initial C12A7-O^- catalyst and (b) the catalyst after the reactions of O^- with benzene for 17 h in the $C_6H_6/O_2/Ar/C12A7\text{-}O^-$ system. By comparing the peak positions and intensities with the data in JCPDS cards, the peaks marked with "*" can be assigned to the structure of C12A7.

are nearly no differences between the diffraction spectra of the initial C12A7-O^- catalyst and the reacted C12A7-O^- catalyst, which demonstrates that the used C12A7-O^- catalyst after the reaction has the same structure of the positively charged lattice framework with the initial catalyst and the reaction does not destroy this structure. The C12A7-O^- catalyst had a long lifetime about 17 h for the benzene conversion, and the stable activity of the C12A7-O^- catalyst would be attributed to its structure stability.

C. Anions species in C12A7-O^-

EPR (Electron Paramagnetic Resonance) measurements were performed to investigate the oxygen species in the bulk of C12A7-O^- catalyst. As shown in Fig.2, for the used C12A7-O^- catalyst, the spectra can be decomposed into two components, and attributed to the oxygen species: O^- (g_{xx}=g_{yy}=2.043 and g_{zz}=1.997) and O_2 (g_{xx}=2.001, g_{yy}=2.010 and g_{zz}=2.070) [17,34-36]. Table II summarizes the concentrations of the anions in the C12A7-O^- cages for the initial C12A7-O^- catalyst and the reacted one under the reaction conditions. The concentrations of the oxygen species in the C12A7-O^- bodies were obtained from the second integral of the EPR spectra using $CuSO_4 \cdot 5H_2O$ as a standard with an error of about 20%. As Table II shows, for initial catalyst, the total concentration of O^- and O_2^- was about 7.0×10^{20} cm^{-3}, while after reaction for 17 h, the total concentration was decreased to 4.2×10^{18} cm^{-3}. The EPR results show that in the C12A7-O^- catalyst after reaction, part of the O^- and O_2^- species translate, and the reformed species in the cages of the reacted C12A7-O^- catalysts should be attributed to other species. Even though OH species cannot be directly detected by the EPR method, the reformed species in the cages of the reacted C12A7-O^- catalysts should be attributed to OH^- due to OH^- existing on the surface (by FT-IR measurements, see below).

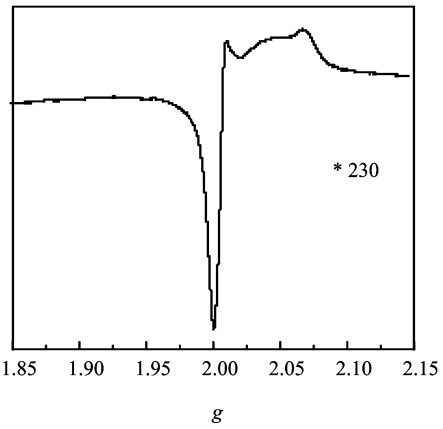

FIG. 2 EPR spectra of the used C12A7-O^- catalyst after the reactions of O with benzene for 17 h in the $C_6H_6/O_2/Ar/C12A7\text{-}O^-$ system. The symbols * 230 in the figure stand for the amplified time of the EPR signal.

TABLE II The anionic concentration in the C12A7-O^- catalysts measured under the reaction conditions.

Species	Concentration/cm^{-3}	
	Before reaction	After reaction[a] for 17 h
$O^- + O_2^-$	7.0×10^{20}	4.2×10^{18}
OH^-	0	$>7.0\times10^{20}$ [b]
Others	8.0×10^{20} [c]	$<8.0\times10^{20}$

[a]Reaction conditions: C_6H_6:O_2:H_2O:Ar=0.08:0.04:0.19:0.69, implantation current: 0.35 mA, flow rate: 63 mL/min, pressure: 101 kPa, C12A7-O^-: 3g.
[b]According to the estimation of the decreased concentration of detected oxygen anions by EPR.
[c]According to the estimation of the theoretical maximum monovalent anion concentration in the lattice framework.

D. Active species on the C12A7-O^- surface

Active species on the C12A7-O^- surface after the reactions in the $C_6H_6/O_2/Ar/C12A7\text{-}O^-$ system were investigated by the Fourier transform infrared (FT-IR) spectra. Fig.3 displays two typical FT-IR spectra obtained by the initial C12A7-O^- catalyst and the catalyst after the reactions for 17 h in the $C_6H_6/O_2/Ar/C12A7\text{-}O^-$ system. The absorption envelopes in the 450-850 cm^{-1} region are attributed to the C12A7 characteristic absorption structures, corresponding to the Al−O stretching and bending modes

DOI:10.1088/1674-0068/20/03/297-304 ©2007 Chinese Physical Society

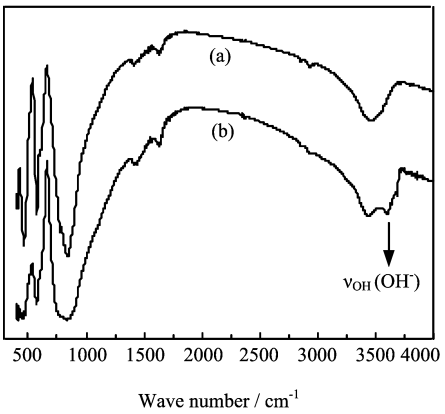

FIG. 3 FT-IR spectra obtained by (a) the initial C12A7-O$^-$ catalyst and (b) the catalyst after the reactions of O$^-$ with benzene for 17 h in the $C_6H_6/O_2/Ar$/C12A7-O$^-$ system.

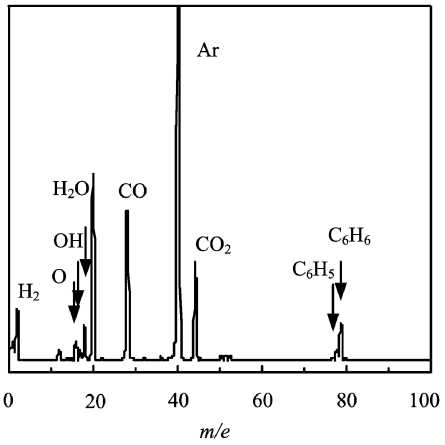

FIG. 4 Typical Q-MS spectrum shows the neutral species for the $C_6H_6/O_2/Ar$/C12A7-O$^-$ system (565 °C, C_6H_6:O_2:Ar=0.08:0.05:0.87, 0.35 mA, 63 mL/min, 101 kPa, C12A7-O$^-$: 3g)

in AlO_4 tetrahedral [37-38]. Even overlapping with a strong 3444 cm^{-1} profile (the water absorption band of the KBr transparent disk), there is a distinguishable and repeatable peak near 3600 cm^{-1}. Because the 3600 cm^{-1} band is close to the ν_{OH}(OH$^-$) [24,39-40], it was assigned to the stretching vibration of O−H$^-$ on the catalyst surface. We found that the 3600 cm^{-1} band only appeared for the reacted C12A7-O$^-$ catalysts in the systems of $C_6H_6/O_2/Ar$/C12A7-O$^-$ and $C_6H_6/O_2/H_2O/Ar$/C12A7-O$^-$. This indicates that the OH$^-$ species adsorbed on the surface were produced during the reactions of the adsorbed benzene with the active O$^-$ by the surface reaction: O$^-$(s)+C_6H_6(s) → C_6H_5(s)+OH$^-$(s), which would play an important role in the benzene conversion and the phenol formation.

E. Neutral species desorbed from C12A7-O$^-$ surface

The neutral products and intermediates in the formation process of phenol were investigated by Q-MS (quadrupole mass spectrometer). The neutral species including H, H_2, O, O_2, OH, CO, CO_2, OH, H_2O, C_6H_5, and C_6H_6, were observed in the $C_6H_6/O_2/Ar$/C12A7-O$^-$ system (C_6H_6:O_2:Ar=0.08:0.05:0.87), as shown in Fig.4. Although some intermediates such as OH and C_6H_5 were detected by Q-MS, it seems difficult to determine if these intermediates result from the dissociation of the parents in the Q-MS system, or formed by the reactions in the process of the phenol synthesis. To study these neutral radicals, we consider using a laser-induced fluorescence method, which will be performed in our future work.

F. Anionic intermediates desorbed from C12A7-O$^-$ surface

To further clarify the formation mechanism of phenol formation from benzene, the benzene conversion reactions were investigated under low-pressure conditions (26.7-40.0 mPa). The anionic species desorbed from the surface of the C12A7-O$^-$ catalyst were detected by TOF-MS (time of flight mass spectrometer). Figure 5 shows the anionic species desorbed from the surface of the fresh C12A7-O$^-$ catalyst. There are two peaks with the respective mass numbers of 16 and 0, which correspond to O$^-$ and electrons, respectively. This indicates that the active O$^-$ appeared on the C12A7-O$^-$ surface, as pointed out by our previous work [18-19,33]. When water was fed onto the C12A7-O$^-$ surface by a nozzle (∼0.04 Pa), the anionic species desorbed from the C12A7-O$^-$ catalyst were different from the initial

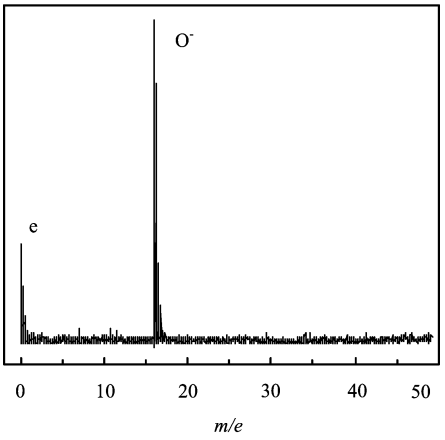

FIG. 5 Typical TOF spectrum shows the O$^-$ anions desorbed from C12A7-O$^-$ (implantation condition: O_2:Ar=0.05:0.95, 266.64 Pa, 0.38 mA, 650 °C).

C12A7-O$^-$ catalyst, as shown in Fig.6. Besides the peaks of O$^-$ and electrons, two new peaks appear around the respective mass numbers of 1 and 17, which are attributed to the anions of H$^-$ and OH$^-$ respec-

DOI:10.1088/1674-0068/20/03/297-304 ©2007 Chinese Physical Society

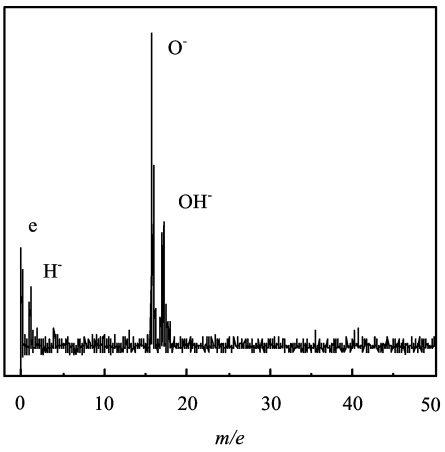

FIG. 6 Typical TOF spectrum shows the O^- and OH^- species desorbed from C12A7-O^- (implantation condition: O_2:H_2O:Ar=0.05:0.20:0.75, 266.64 Pa, 0.38 mA, 650 °C).

tively. The formation of OH^- is suggested by the following surface reaction:

$$O^-(s) + H_2O(s) \longrightarrow OH(s) + OH^-(s) \quad (1)$$

where "s" stands for the catalyst surface.

Fig.7 shows a TOF spectrum, as benzene (∼0.04 Pa) was injected onto the C12A7-O^- surface. The spectrum became complex, and a series of new peaks appeared. The reproducible peaks with the respective mass numbers of 1, 12, 13, 14, 16, 17, 18, 24, 25, 28, 44, 76, 77, 93, and 94, are attributed to the desorbed anions of H^-, C^-, CH^-, $CH_2{}^-$, O^-, OH^-, H_2O^-, $C_2{}^-$, C_2H^-, CO^-, $CO_2{}^-$, $C_6H_4{}^-$, $C_6H_5{}^-$, $C_6H_5O^-$, and $C_6H_5OH^-$, respectively. The anionic hydrocarbons are believed to be generated by the decomposition of benzene followed by the charge-transfer reactions with O^-. The anionic oxides are expected to form by the reactions of O^- with the dissociation fragments. It is noted that there are two stronger peaks of OH^- and $C_6H_5OH^-$, which are suggested by following reactions:

$$O^-(s) + C_6H_6(s) \longrightarrow C_6H_5(s) + OH^-(s) \quad (2)$$

$$C_6H_6(s) \longrightarrow C_6H_5(s) + H(s) \quad (3)$$

$$C_6H_5(s) + OH^-(s) \longrightarrow C_6H_5OH^-(s) \quad (4)$$

When the benzene/oxygen/water mixture was supplied onto the C12A7-O^-, it was found that both OH^- and $C_6H_5OH^-$ intensity increased (Fig.8). The OH^- was generated from reaction (1) as water was fed. The increase of the $C_6H_5OH^-$ intensity could be caused by the increase of OH^- concentration on the catalyst's surface. The role of water in the reaction system may be to enhance hydroxylation of benzene by increasing OH and OH^- concentration, and inhibit the consequent oxidation of phenol.

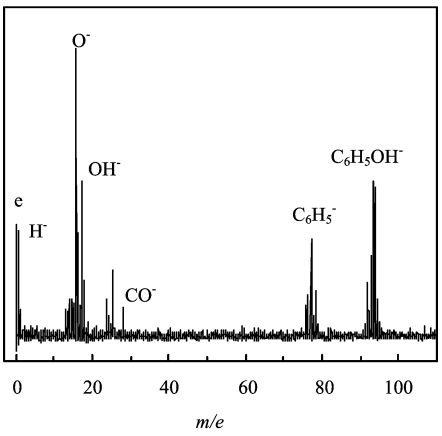

FIG. 7 TOF spectrum for the C_6H_6:Ar:C12A7-O^- reaction system. C_6H_6: 0.04 Pa, 0.38 mA, 650 °C

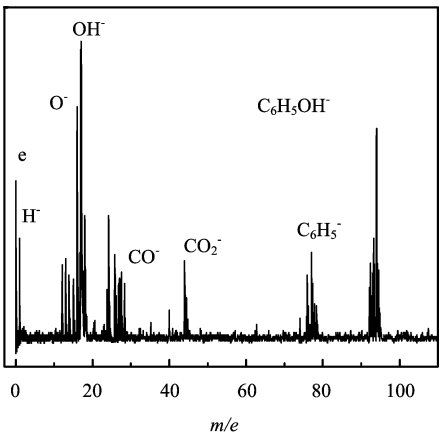

FIG. 8 TOF spectra for three reaction systems: $C_6H_6/O_2/H_2O$/Ar/C12A7-O^-. C_6H_6: 0.04 Pa, 0.38 mA, 650 °C, O_2/H_2O/Ar=0.05:0.20:0.75 were supplied onto the backside of C12A7-O^-.

G. Mechanism of phenol formation on C12A7-O^-

To facilitate the discussion of the results and the mechanism of phenol formation from $C_6H_6/O_2/H_2O$ on C12A7-O^-, we first summarize the main observations:

(i) The benzene conversion over C12A7-O^- catalyst mainly depends on the reaction temperature. The phenol selectivity and the yield are mainly affected by the reaction temperature and the composition of the feeding mixture (i.e. the ratio of C_6H_6:H_2O:O_2). Addition of water significantly increases the phenol selectivity. The optimum synthesis conditions are at about 565 °C and C_6H_6:O_2:H_2O=2:1:4.8, where the benzene conversion is 34% with a high phenol selectivity of about 90%. Additionally, it was found that carbon deposition was negligible after 1000 min's reaction.

(ii) The synthesis reactions do not destroy the positively charged framework of C12A7-O^- (i.e. cage structure). The stable activity of the C12A7-O^- catalyst can be attributed to its structure stability.

DOI:10.1088/1674-0068/20/03/297-304 ©2007 Chinese Physical Society

(iii) After the synthesis reactions, a part of the oxygen species (O^-(cage) and $O_2{}^-$(cage)) in the C12A7-O^- bodies were replaced by the species of OH^-(cage).

(iv) The surface species of OH^-(s) were formed in the synthesis reactions, generated by the reactions of O^-(s) with water and benzene.

(v) The OH^- (gas-phase) and $C_6H_5OH^-$ (gas-phase) anionic species observed were formed by the surface reactions of O^-(s) with the adsorbed benzene, and then desorbed into the gas phase.

It is well known that the structure of C12A7, containing two molecules per unit cell, is characterized by a positively charged lattice framework $[Ca_{24}Al_{28}O_{64}]^{4+}$ having 12 crystallographic cages per unit cell with a free space of ∼0.4 nm in diameter. The remaining two oxide ions ($O_2{}^-$), referred to as "free oxygen", are clathrated in the cages to maintain charge neutrality [17]. With this special structure of C12A7, we have confirmed that the mono-charge anions of X^- (X^-=O^-, OH^-, and H^- etc.) can be substituted for free oxygen, and form a series of new C12A7-X materials [18,19]. A sustainable and stable O^- emission current can be obtained from this C12A7-O^- material by continuously supplying O_2 and electrons onto the C12A7-O^- catalyst. On the other hand, while continuously supplying H_2O and electrons onto the C12A7-O^- catalyst, a sustainable OH^- emission of several $\mu A/cm^2$ was also observed with the prolongation of operating time. As the mixed-gas $O_2/H_2O/Ar$ and electrons was implanted onto the C12A7-O^-, a simultaneous emission of O^- together with OH^- from the C12A7-O^- catalyst was observed [33].

According to the structure characteristics of C12A7-O^- and the most important features of encaging and desorbing O^- and OH^-, the active oxygen species of O^- and OH^- must play a key role in the phenol formation from $C_6H_6/O_2/H_2O$. The present results also confirmed that the OH^- species appeared both on the catalyst surface and in the cages of C12A7-O^- after the reactions of benzene with O^-(s) by Eqs.(1) and (2). Thus, the formation of phenol can be correlated with the active species of O^-(s) and OH^-(s). O^-(s) is suggested as an active species in initiating the benzene conversion process via hydrogen abstraction reaction through Eq.(2) because OH^-, both on the surface and in the gas phase, was observed as benzene was fed into C12A7-O^-. Then the intermediate species $C_6H_5OH^-$(s) was formed from the phenyl radical C_6H_5(s) and OH^-(s), leading to the formation of phenol by an electron detachment process. The above mechanism was mainly based on the following observations: (i) O^-(s)and OH^-(s) were found on the C12A7-O^- surface, (ii) $C_6H_5OH^-$ was observed in the reaction system of C_6H_6/C12A7-O^-, (iii) with increasing amounts of OH^-, the intensity of $C_6H_5OH^-$ increased; (iv) the phenol selectivity and yield was enhanced by addition of water. Thus, we suggest the phenol formation occurs by the following main surface reaction processes:

$$C_6H_6(s) + O^-(s) \longrightarrow C_6H_5(s) + OH^-(s) \quad (5)$$

$$H_2O(s) + O^-(s) \longrightarrow OH(s) + OH^-(s) \quad (6)$$

$$C_6H_6(s) \longrightarrow C_6H_5(s) + H(s) \quad (7)$$

$$C_6H_5(s) + OH^-(s) \longrightarrow C_6H_5OH^-(s) \quad (8)$$

$$C_6H_5OH^-(s) \longrightarrow C_6H_5OH(g) \uparrow + e^-(s) \quad (9)$$

where "s" stands for the catalyst surface.

Moreover, by separating the emission zone (C12A7-O^- source) from the reaction zone (the feeding area of benzene), no $C_6H_5OH^-$ and phenol can be detected. This indicates that the phenol produced by the gas-phase reactions between O^- and benzene seems negligible, and the benzene conversion and phenol formation are caused by the surface reactions over the C12A7-O^- catalyst.

IV. CONCLUSION

Direct conversion of benzene to phenol by O_2/H_2O over the synthesized $[Ca_{24}Al_{28}O_{64}]^{4+}\cdot 4(O^-)$ (C12A7-O^-) catalyst was obtained. A benzene conversion rate of 34% with phenol selectivity about 90% was obtained at 565 °C and the mixture ratio of C_6H_6:O_2:H_2O=2:1:4.8. Carbon formation was found to be negligible after 1000 min's reaction. The synthesis reactions do not destroy the positively charged framework of the C12A7-O^-. After the synthesis reactions, part of the oxygen species (O^-(cage) and $O_2{}^-$(cage)) in the C12A7-O^- bulk was replaced by the species OH^-(cage). The surface species OH^-(s) is formed in the synthesis reactions, generated by the reactions of O^-(s) with water and benzene. The OH^- (gas-phase) and $C_6H_5OH^-$ (gas-phase) anionic species observed are formed by the surface reactions of O^-(s) with the adsorbed benzene and then desorbed into the gas phase. O^-(s) is suggested as an active species in initiating the benzene conversion process via hydrogen abstraction reaction. Then, the intermediate species $C_6H_5OH^-$(s) was formed from the phenyl radical C_6H_5(s) and OH^-(s), leading to the formation of phenol by an electron detachment process.

V. ACKNOWLEDGMENTS

We thank Prof. Y. L. Fu and P. Y. Lin for their helpful discussions. This work was supported by the "Bairen Program of Chinese Academy of Sciences 2002" and the "Innovation Program of Chinese Academy of Sciences 2002".

DOI:10.1088/1674-0068/20/03/297-304 ©2007 Chinese Physical Society

[1] Y. C. Yen, *Process Economics Program, Stanford Research Institute International*, Carlifornia: Menlo Park, (1967).
[2] M. Iwamoto, J. Hirata, K. Matsukami, and S. Kagawa, J. Phys. Chem. **87**, 903 (1983).
[3] A. Reitzmann, E. Klemm, and G. Emig, Chem. Eng. J. **90**, 149 (2002).
[4] G. I. Panov, A. K. Uriarte, M. A. Rodkin, and V. I. Sobolev, Catal. Today **41**, 365 (1998).
[5] G. I. Panov, Cattech, **4**, 18 (2000).
[6] G. I. Panov, G. A. Sheveleva, A. S. Kharitonov, V. N. Rommanikov, and L. A. Vostrikova, Appl. Catal. **82**, 31 (1992).
[7] D. P. Ivanov, M. A. Rodkin, K. A. Dubkov, A. S. Kharitonov, and G. I. Panov, Kinet. Catal. **41**, 771 (2000).
[8] V. I. Sobolev, A. S. Kharitonov, Y. A. Paukshtis, and G. I. Panov, J. Mol. Catal. **84**, 117 (1993).
[9] J. L. Motz, H. Heinichen, and W. F. Hölderich, J. Mol. Catal. A: Chem. **136**, 175 (1998).
[10] A. S. Kharitonov and G. I. Panov, US Patent 05672777, (1996).
[11] C. W. Lee, W. J. Lee, Y. K. Park, and S. E. Park, Catal. Today **61**, 137 (2000).
[12] K. Fujishima, A. Fukuoka, A. Yamagishi, S. Inagak, Y. Fukushima, and M. Ichikawa, J. Mol. Catal. A **166**, 211 (2001).
[13] V. I. Parvulescu, D. Dimitriu, and G. Poncelet, J. Mol. Catal. **140**, 91 (1999).
[14] A. Thangaraj, R. Kumar, and P. Ratnasamy, Appl. Catal. **57**, L1 (1990).
[15] S. I. Niwa, M. Eswaramoorthy, J. Nair, A. Raj, N. Itoh, H. Shoji, T. Namba, and F. Mizukami, Science **295**, 105 (2002).
[16] A. Kunai, T. Wani, Y. Uehara, F. Iwasaki, Y. Kuroda, S. Ito, and K. Sasaki, Bull. Chem. Soc. Jpn. **62**, 2613 (1989).
[17] K. Hayashi, M. Hirano, S. Matsuishi, and H. Hosono, J. Am. Chem. Soc. **124**, 738 (2002).
[18] Q. X. Li, H. Hosono, M. Hirano, K. Hayashi, M. Nishioka, H. Kashiwagi, Y. Totimoto, and M. Sadakata, Surf. Sci. **527**, 100 (2003).
[19] Q. X. Li, K. Hayashi, M. Nishioka, H. Kashiwagi, M. Hirano, H. Hosono, and M. Sadakata, Appl. Phys. Lett. **80**, 4259 (2002).
[20] D. V. Deubel and G. Frenking, J. Am. Chem. Soc. **121**, 2021 (1999).
[21] R. W. Fessenden and D. Meisel, J. Am. Chem. Soc. **122**, 3773 (2000).
[22] J. Lee and J. J. Grabowski, Chem. Rev. **92**, 1611 (1992).
[23] M. Born, S. Ingemann, and N. M. M. Nibbering, Mass Spectrom. Rev. **16**, 181 (1997).
[24] T. Tashiro, T. Watanabe, M. Kawasaki, and K. Toi, J. Chem. Soc. Faraday Trans. **89**, 1263 (1993).
[25] K. I. Aika and J. H. Lunsford, J. Phys. Chem. **81**, 1393 (1977).
[26] T. Ito, T. Tashiro, M. Kawasaki, T. Watanabe, and K. Toi, J. Phys. Chem. **95**, 4476 (1991).
[27] S. G. Neophytides, D. Tsiplakides, P. Stonehart, M. M. Jaksic, and C. G. Vayenas, Nature **370**, 45 (1994).
[28] J. H. Lunsford, Adv. Catal. **22**, 265 (1972).
[29] M. A. Goula, A. A Lemonidou, W. Grünert, and M. Baerns, Catal. Today **32**, 149 (1996).
[30] H. Xian, Y. Pan, S. B. Qiu, J. Tu, X. F. Zhu, and Q. X. Li, Chin. J. Chem. Phys. **18**, 469 (2005).
[31] Y. Pan, Z. X. Wang, T. Kan, X. F. Zhu, and Q. X. Li, Chin. J. Chem. Phys. **19**, 190 (2006).
[32] T. Dong, J. Li, F. Huang, L. Wang, J. Tu, Y. Torimoto, M. Sadakata, and Q. X. Li, Chem. Comm. **21**, 2724 (2005)..
[33] J. Li, F. Huang, L. Wang, S. Q. Yu, Y. Torimoto, M. Sadakata, and Q. X. Li, Chem. Mater. **17**, 2771 (2005).
[34] K. Hayashi, S. Matsuishi, N. Ueda, M. Hirano, and H. Hosono, Chem. Mater. **15**, 1851 (2003).
[35] S. Yang, J. N. Konda, K. Hayashi, M. Hirano, K. Domen, and H. Hosono, Chem. Mater. **16**, 104 (2004).
[36] H. Hosono and Y. Abe, Inorg. Chem. **26**, 1192 (1987).
[37] P. Tarte, Spectrochim. Acta A **23A**, 2127 (1967).
[38] R. A. Schroeder, and L. L. Lyons, J. Inorg. Nucl. Chem. **28**, 1155 (1966).
[39] R. K. Datta, J. Am. Ceram. Soc. **70**, C288 (1987).
[40] B. Henderson and W. A. Sibley, J. Chem. Phys. **55**, 1276 (1971).

DOI:10.1088/1674-0068/20/03/297-304 ©2007 Chinese Physical Society